

Self-Doping of Gold Chains on Silicon: A New Structural Model for Si(111)5×2-Au

Steven C. Erwin

Center for Computational Materials Science, Naval Research Laboratory, Washington, D.C. 20375

(Dated: November 13, 2018)

A new structural model for the Si(111)5×2-Au reconstruction is proposed and analyzed using first-principles calculations. The basic model consists of a “double honeycomb chain” decorated by Si adatoms. The 5×1 periodicity of the honeycomb chains is doubled by the presence of a half-occupied row of Si atoms that partially rebonds the chains. Additional adatoms supply electrons that dope the parent band structure and stabilize the period doubling; the optimal doping corresponds to one adatom per four 5×2 cells, in agreement with experiment. All the main features observed in scanning tunneling microscopy and photoemission are well reproduced.

PACS numbers: 68.43.Bc, 73.20.At, 68.35.Bs, 81.07.Vb

Physical realizations of a one-dimensional metal are rare, in part because they may be preempted by a metal-insulator Peierls transition [1]. An escape clause is available for metallic chains adsorbed on rigid substrates, however, since the energy penalty for the pairing distortion may be prohibitively high. For example, when gold is adsorbed on silicon a variety of chain-like structures are formed, some with unusual electronic properties suggestive of a one-dimensional metal [2, 3]. Photoemission data from the vicinal surfaces Si(553)-Au and Si(557)-Au reveal fractionally filled bands with strongly one-dimensional character, which are believed to originate from Au “chains” just one atom wide [4]. Structural models for Si(557)-Au were recently proposed based on total-energy calculations [5] and x-ray data [6].

Even more widely studied is the parent flat surface, Si(111)-Au. First reported over twenty-five years ago [7, 8], the Si(111)5×2-Au reconstruction has been extensively characterized by low-energy electron diffraction [8, 9], scanning tunneling microscopy (STM) [10, 11, 12], x-ray diffraction [13], reflectance anisotropy spectroscopy [14], angle-resolved photoemission [15, 16], inverse photoemission [17], and core-level spectroscopy [18]. Despite this scrutiny, its structure remains unknown. The data provide several constraints on any model of Si(111)5×2-Au. (1) STM shows the surface to be decorated by bright protrusions with apparent height ~ 1.5 Å and whose coverage, although variable, has a preferred value of one per 5×8 supercell [19]. (2) Away from the protrusions, STM images show a “Y”-shaped feature whose orientation is determined by the underlying lattice [11, 12, 14]. (3) Photoemission finds a strong surface band beginning at the the 5×2 zone boundary and dispersing downward toward the 5×1 zone boundary [16]. (4) The nature of this band changes from one-dimensional at the top of the band to two-dimensional at its bottom [20].

In this Letter a new model is proposed for Si(111)5×2-Au that explains all of these observed features. The model is related to those proposed earlier for Si(557)-Au, suggesting that all of the reconstructions formed by adsorption of Au on Si form a family. It is also closely

related to the “honeycomb chain-channel” (HCC) model now widely accepted as the structure of the adsorbate-induced induced Si(111)3×1 and Si(111)3×2 reconstructions [21], and thus helps to unify a wide class of adsorbate-induced reconstructions based on Si(111) and its vicinals. The present model achieves its stability through an unusual “self-doping” mechanism that may be relevant to other Au-induced Si reconstructions.

The model is shown in Fig. 1. The reconstruction oc-

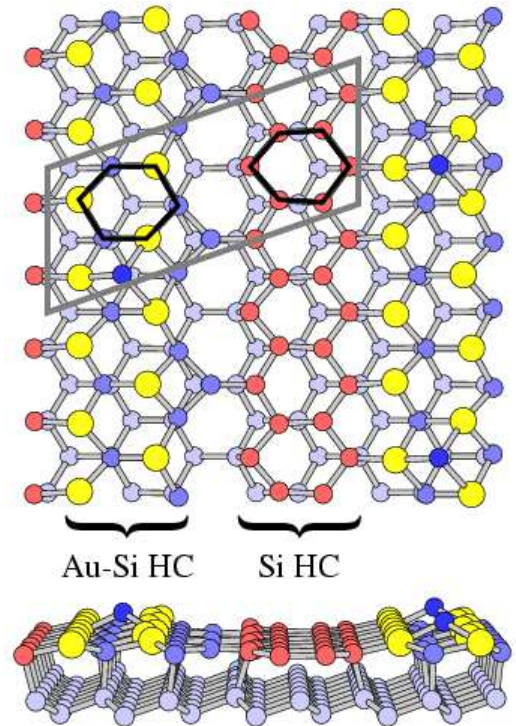


FIG. 1: (color) Proposed “double honeycomb chain” structure of Si(111)5×2-Au. Large circles are Au, small circles are Si. The elementary 5×2 unit cell is outlined. Each unit cell contains two honeycomb chains (HC) based on the outlined hexagons, one of alternating Au and Si atoms, the other of all Si. Three additional Si adatoms, with 5×4 periodicity, are also shown (see discussion).

curs purely in the surface layer, and has the basic structure of a “double honeycomb chain” (DHC) with underlying 5×1 periodicity. One chain is formed by hexagons of alternating Au and Si atoms, and one by hexagons of all Si (as in the HCC model). The outer Si atoms of the Au-Si chain are too far from the Si atoms in the Si chain to bond directly. As a result, two variants of the basic model are plausible. (i) The insertion of an additional “rebonding” row of Si atoms can bridge the gap between the chains, but only at the cost of overcoordinating the Si atoms in the Au-Si chain. This will be called the “ 5×1 variant.” (ii) Removing every other of these rebonding Si atoms (as shown in Fig. 1) relieves the overcoordination but now leaves dangling bonds in the Si chain; this will be called the “ 5×2 variant.” These two variants are very close energetically. It will be shown below that the presence of additional Si, occurring as adatoms, acts to dope the 5×2 variant with electrons and thereby to reduce its surface energy relative to the 5×1 variant. The optimal doping level occurs for one adatom per four 5×2 cells, identical to the observed equilibrium adatom coverage.

First-principles total-energy calculations were used to determine the equilibrium geometries and relative surface energies of the basic model and its variants. The calculations were performed in a slab geometry with up to six layers of Si plus the reconstructed surface layer and a vacuum region of 8 Å. All atomic positions were relaxed until the total energy changed by less than 1 meV per 5×2 cell; the bottom Si layer was passivated by hydrogen and held fixed. Total energies and forces were calculated within the generalized-gradient approximation to density-functional theory using projector-augmented-wave potentials, as implemented in VASP [22, 23]. The plane-wave cutoff (180 eV) and sampling (2×4) of the surface Brillouin zone were sufficient to converge relative surface energies to within 1 meV/Å², adequate for the comparisons presented below. All the models considered here have equal Au coverage, and hence the relative surface energies (calculated as in Ref. 21) do not require a choice of Au chemical potential. STM images were simulated using the method of Tersoff and Hamann [24].

Since its discovery, many structural models have been proposed for Si(111) 5×2 -Au. Most of the early ones are not compatible with newer STM data, but two later models—from Marks and Plass (MP) [25] and Hasegawa, Hosaka, and Hosoki (HHH) [26]—have recently been studied theoretically [27]. Neither was found to be consistent with STM or ARPES data, despite being locally stable with nearly equal surface energies (to within 0.1 meV/Å²). The 5×2 DHC model proposed here is more stable than the MP and HHH models by 20 meV/Å², or 2.6 eV per 5×2 cell. This energy difference is sufficiently large to rule out the MP and HHH models on energetic grounds alone.

Within the family of the two DHC variants described above (5×1 versus 5×2 , each with different Si adatom

coverages) the relative surface energy changes are very much smaller, of order 1 meV/Å². This is near the limiting precision for DFT surface energies, suggesting the need for a simpler model to describe, for example, the variation of surface energy with Si adatom coverage. In the following, this model is developed by analyzing within DFT the role of the adatoms. This requires demonstrating, first, that the observed bright protrusions in STM are, in fact, Si adatoms and not something else; and second, that the adatoms indeed supply electrons, which

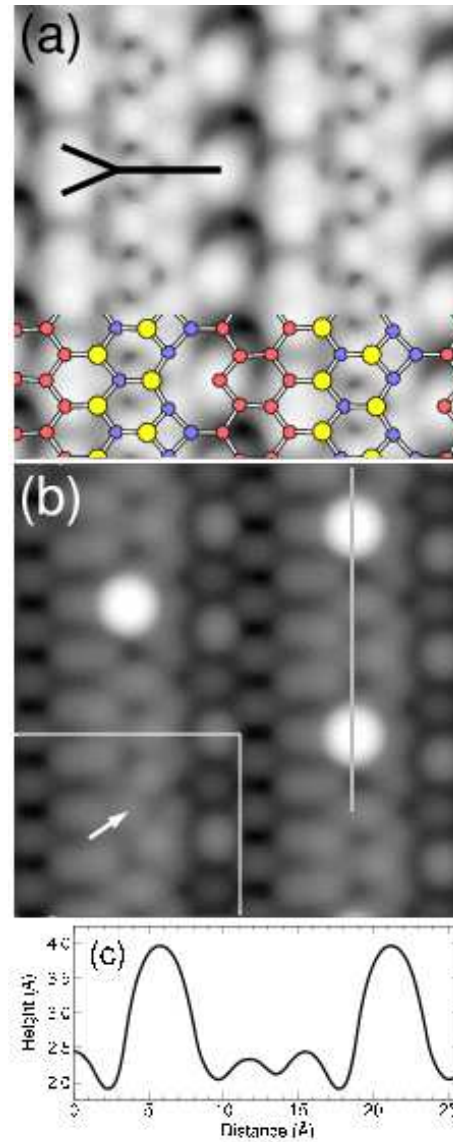


FIG. 2: (color) Simulated filled-state STM images for double honeycomb chain model. (a) Image for 5×2 model (sample bias -0.8 V), showing “Y”-shaped feature observed in Ref. 11. (b) Same surface, with adsorbed Si atoms as in Fig. 1 (sample bias -2.0 V), showing bright protrusions observed in Ref. 19. Inset: simulated image from an adsorbed Au atom at the same in-plane location (marked by arrow). (c) Linescan through two bright protrusions, as marked in panel (b).

then dope the parent band structure.

Away from the protrusions, filled-state STM images show a series of side-by-side “Y”-shaped features with 5×2 periodicity [11, 12, 14]. A simulated STM image for the 5×2 DHC model with no adatoms is shown in Fig. 2(a). A similar feature “Y”-shaped feature is found with paired “arms,” a single “tail,” and the same crystallographic orientation as found experimentally.

To identify the bright protrusions seen in STM images, both Si and Au adatoms were considered as potential candidates. Binding energies for individual adatoms were calculated for eight possible sites on the undecorated 5×2 surface. For Si the most favorable site is at the center of a Au-Si hexagon, as shown in Fig. 1, where the binding energy is 4.6 eV. This is much larger than the next best site (by 0.7 eV) and hence rules out other possible locations. The simulated STM image, shown in Fig. 2(b), from a 5×4 arrangement of Si adatoms decorating these sites is in excellent agreement with the atomically resolved images of Ref. [19]. In particular, the bright spots are correctly positioned in the middle of the underlying row structures. The linescan in Fig. 2(c) shows their apparent height to be 1.5 Å, in good agreement with the results of Ref. [19]. Finally, Au adatoms can be easily ruled out as plausible candidates: although their binding energies are substantial (from 3.1 to 3.9 eV), they relax well into the surface layer and thus produce no detectable STM spot, as demonstrated in the inset to Fig. 2(b).

Photoemission data for Si(111) 5×2 -Au provide a very stringent test for any structural model. For wavevectors along the chain direction, the ARPES data reveal a strong surface band beginning at the 5×2 zone boundary (the A_2 point), and dispersing downward to its minimum at the 5×1 zone boundary (the A_1 point) before turning back up [16]. The calculated electronic structure, shown in Fig. 3, reveals just such a band between A_2 and A_1 , whose width and effective mass (0.6 eV and $0.4m_e$) are in reasonably good agreement with the data (0.9 eV and $0.5m_e$). Additional bands with less pronounced surface character are also found in the data, and can be tentatively identified with calculated bands marked in Fig. 3.

One remarkable feature of the ARPES results for the strong surface band is the continuous transition, within a single band, from a one-dimensional state (at the band maximum) to a two-dimensional state (at its minimum) [20]. This feature is well reproduced in the calculated band structure, expanded views of which are shown in the two small panels of Fig. 3 for wavevectors perpendicular to the chain direction. At the maximum of the strong band, near A_2 , the perpendicular dispersion is small (0.04 eV), while at its minimum, near A_1 , the perpendicular dispersion is much larger (0.10 eV). The ARPES measurements give very similar results, 0.03 ± 0.03 eV and 0.14 ± 0.03 eV, respectively [20].

It is clear from Fig. 3 that the calculated electronic structure of the bare Si(111) 5×2 -Au reconstruction is

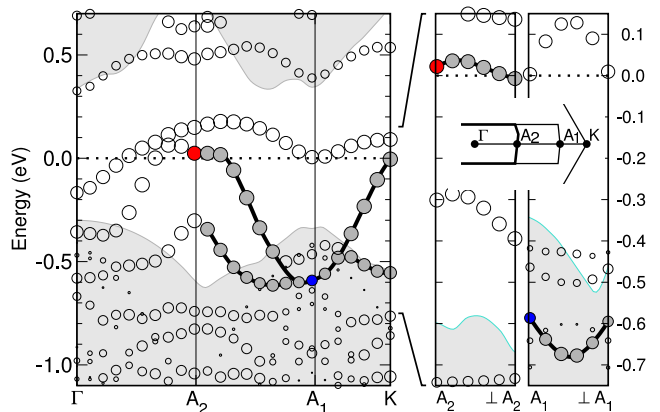


FIG. 3: (color) Band structure of 5×2 double honeycomb chain model with no adatoms. The size of each circle reflects the surface character of the state (radii are proportional to the total charge in spheres around surface-layer atoms). The shaded states form bands that are detected in photoemission data (see discussion). Left panel and right panels show dispersion along and perpendicular to chain direction, respectively. The colored circles in the left and right panels mark the same states; note the change of energy scale.

metallic. As suggested in Ref. [1], it is interesting to ask whether the addition of Si adatoms could render the system either insulating, or at least “less metallic”; whether it is energetically favorable to do so; and—if it is—whether the predicted optimal coverage of adatoms corresponds to the equilibrium coverage deduced from STM data, one per 5×8 supercell [19]. The answer to all three questions is affirmative, as shown below.

Near the Fermi level the bands are very close to one-dimensional, as discussed above. Hence, the number of additional electrons required to render the band structure (provisionally assumed to be rigid) insulating can be trivially determined from Fig. 3 to be two per 5×2 cell. To determine what coverage of Si adatoms is required to provide two electrons per 5×2 cell, explicit band structure calculations must be performed. For a coverage of one adatom per 5×2 cell, the resulting band structure is insulating. This implies that the addition of one adatom to the bare 5×2 surface creates only one additional state in the occupied manifold: two of the adatom’s valence electrons fill this state, and the other two dope the parent band structure, rendering the full system insulating. These conclusions are independent of any assumptions about the rigidity of the parent band structure. Nevertheless, it is important to note that the bands do shift quite rigidly, with only small changes of order 0.1 eV or less. For lower adatom coverages, smaller but similarly rigid shifts are expected. This transforms the determination of the optimal adatom coverage into the equivalent task of computing the optimal electron doping.

In the absence of adatoms, the DFT surface energies of the 5×1 and 5×2 DHC models are very close,

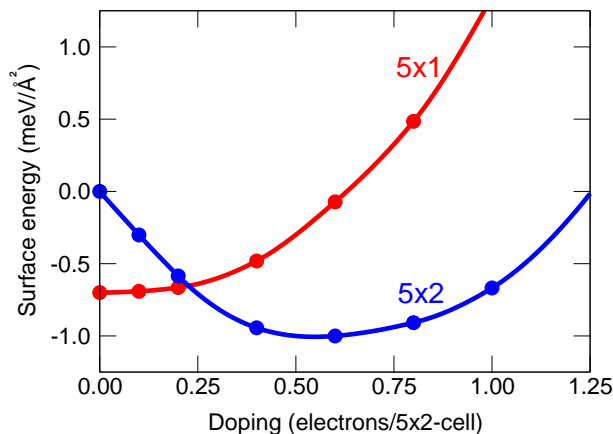


FIG. 4: Variation of surface energy with electron doping, for 5×1 and 5×2 models. The most favorable structure has 5×2 periodicity with 0.5 extra electron per 5×2 cell.

with the 5×1 variant preferred by less than $1 \text{ meV}/\text{\AA}^2$. Changes in the surface energy due to electron doping were modeled by calculating the DFT total energies for cells with additional electronic charge (with a compensating background charge to preserve overall neutrality, plus the standard correction to treat the resulting spurious interactions [28]). The results are shown in Fig. 4. For the 5×1 variant, any additional electronic charge increases the surface energy above its undoped value. The 5×2 variant behaves quite differently: its surface energy is minimized for a doping level very close to 0.5 electron per 5×2 cell. Since each adatom was earlier shown to supply two doping electrons per 5×2 cell, this optimal doping level can be most easily achieved with one adatom per four 5×2 cells. Moreover, at this optimal adatom coverage the surface energy of the 5×2 variant is lower than that of the 5×1 , suggesting that this is indeed the observed ground-state equilibrium phase [29]. These findings are in excellent agreement with the experimental observation that when excess Si is evaporated at low temperature onto a $\text{Si}(111)5\times 2\text{-Au}$ surface with one adatom per four 5×2 cells, subsequent annealing at higher temperature will cause the extra Si to diffuse away and return the system to its equilibrium state.

In summary, a new structural model has been proposed for the $\text{Si}(111)5\times 2\text{-Au}$ surface, consisting of a “double honeycomb chain” reconstruction decorated by Si adatoms. Simulated STM images from this model reproduce a number of experimentally observed features, including the in-plane location and apparent height of the bright protrusions due to the adatoms, and the “Y”-shaped features seen away from these protrusions. The calculated band structure reproduces the main features of recent photoemission data, including the unusual change in dimensionality observed within the main surface band between its energy extrema. Finally, the Si adatoms act as electron donors that dope the parent 5×2 band struc-

ture, reducing its surface energy and stabilizing it relative to other models. The optimal doping level is equivalent to one Si adatom per four 5×2 cells, in agreement with experimental observation.

Many helpful conversations with F.J. Himpsel are gratefully acknowledged. Computations were performed at the DoD Major Shared Resource Center at ASC. This work was supported by the Office of Naval Research.

-
- [1] F. J. Himpsel, K. N. Altmann, J. N. Crain, A. Kirakosian, J. L. Lin, A. Liebsch, and V. P. Zhukov, *J. Electron Spectroscopy and Related Phenomena* **126**, 89 (2002).
 - [2] P. Segovia, D. Purdie, M. Hengsberger, and Y. Baer, *Nature* **402**, 504 (1999).
 - [3] R. Losio, K. N. Altmann, A. Kirakosian, J.-L. Lin, D. Y. Petrovykh, and F. J. Himpsel, *Phys. Rev. Lett.* **86**, 4632 (2001).
 - [4] J. N. Crain, A. Kirakosian, K. N. Altmann, C. Bromberger, S. C. Erwin, J. McChesney, J.-L. Lin, and F. J. Himpsel, *Phys. Rev. Lett.* **90**, 176805 (2003).
 - [5] D. Sanchez-Portal, J. D. Gale, A. Garcia, and R. M. Martin, *Phys. Rev. B* **65**, 081401 (2002).
 - [6] I. K. Robinson, P. A. Bennett, and F. J. Himpsel, *Phys. Rev. Lett.* **88**, 096104 (2002).
 - [7] H. Lipson and K. E. Singer, *J. Phys. C* **7**, 12 (1974).
 - [8] G. LeLay and J. P. Faurie, *Surf. Sci.* **69**, 295 (1977).
 - [9] H. E. Bishop and J. C. Riviere, *British Journal of Applied Physics* **2**, 1635 (1969).
 - [10] A. A. Baski, J. Nogami, and C. F. Quate, *Phys. Rev. B* **41**, 10247 (1990).
 - [11] J. D. O’Mahony, C. H. Patterson, J. F. McGilp, F. M. Leibsle, P. Weightman, and C. F. J. Flipse, *Surf. Sci.* **277**, L57 (1992).
 - [12] J. D. O’Mahony, J. F. McGilp, C. F. J. Flipse, P. Weightman, and F. M. Leibsle, *Phys. Rev. B* **49**, 2527 (1994).
 - [13] C. Schamper, W. Moritz, H. Schulz, R. Feidenhans’l, M. Nielsen, F. Grey, and R. L. Johnson, *Phys. Rev. B* **43**, 12130 (1991).
 - [14] J. R. Power, P. Weightman, and J. D. O’Mahony, *Phys. Rev. B* **56**, 3587 (1997).
 - [15] I. R. Collins, J. T. Moran, P. T. Andrews, R. Cosso, J. D. O’Mahony, J. F. McGilp, and G. Margaritondo, *Surf. Sci.* **325**, 45 (1995).
 - [16] K. N. Altmann, J. N. Crain, A. Kirakosian, J.-L. Lin, D. Y. Petrovykh, F. J. Himpsel, and R. Losio, *Phys. Rev. B* **64**, 035406 (2001).
 - [17] I. G. Hill and A. B. McLean, *Appl. Surf. Sci.* **123-124**, 371 (1998).
 - [18] H. M. Zhang, T. Balasubramanian, and R. I. G. Uhrberg, *Phys. Rev. B* **65**, 035314 (2002).
 - [19] R. Bennewitz, J. N. Crain, A. Kirakosian, J.-L. Lin, J. L. McChesney, D. Y. Petrovykh, and F. J. Himpsel, *Nanotechnology* **13**, 499 (2002).
 - [20] R. Losio, K. N. Altmann, and F. J. Himpsel, *Phys. Rev. Lett.* **85**, 808 (2000).
 - [21] S. C. Erwin and H. H. Weitering, *Phys. Rev. Lett.* **81**, 2296 (1998).
 - [22] G. Kresse and J. Hafner, *Phys. Rev. B* **47**, 558 (1993).
 - [23] G. Kresse and J. Furthmüller, *Phys. Rev. B* **54**, 11169

- (1996).
- [24] J. Tersoff and D. R. Hamann, Phys. Rev. B **31**, 805 (1985).
- [25] L. D. Marks and R. Plass, Phys. Rev. Lett. **75**, 2172 (1995).
- [26] T. Hasegawa, S. Hosaka, and S. Hosoki, Surf. Sci. **357-358**, 858 (1996).
- [27] M.-H. Kang and J. Y. Lee, Surf. Sci. **531**, 1 (2003).
- [28] G. Makov and M. C. Payne, Phys. Rev. B **51**, 4014 (1995).
- [29] This analysis neglects other contributions to the energy, but these are expected to be small since the DFT surface energy changes by only $1 \text{ meV}/\text{\AA}^2$ upon adding one adatom per 5×2 cell.